The growth and morphogenesis of the gastropod shell

Adam B. Johnson[a]
Nina S. Fogel[b]
J. David Lambert[a,1]

[a]Department of Biology, University of Rochester, Rochester NY 14627, USA
[b]Department of Biology, Saint Louis University, St. Louis, MO 63103, USA
[1]Corresponding Author (Email: dlamber2@mail.rochester.edu)

Abstract

Gastropod shell morphologies are famously diverse but generally share a common geometry, the logarithmic coil. Variations on this morphology have been modeled mathematically and computationally but the developmental biology of shell morphogenesis remains poorly understood. Here we characterize the organization and growth patterns of the shell-secreting epithelium of the larval shell of the basket whelk *Tritia* (a.k.a. *Ilyanassa*). Despite the relative simplicity of the larval shell, we find a surprisingly complex organization of the shell margin in terms of rows and zones of cells. We examined cell division patterns with EdU incorporation assays and found two growth zones within the shell margin. In the more anterior aperture growth zone (AGZ), we find that inferred division angles are biased to lie parallel to the shell edge, and that these divisions occur more on the margin's left side. In the more posterior mantle epithelium growth zone (MEGZ), inferred divisions are significantly biased to the right relative to the anterior-posterior axis. These growth zones, and the left-right asymmetries in cleavage patterns they display can explain the major modes of shell morphogenesis at the level of cellular behavior. In a gastropod with a different coiling geometry, *Planorbella* sp., we find similar shell margin organization and growth zones as *Tritia*, but different left-right asymmetries than we observed in the helically coiled shell of *Tritia*. These results indicate that differential growth patterns in the mantle edge epithelium contribute to shell shape in gastropod shells and identify cellular mechanisms that may vary to generate shell diversity in evolution.

Significance statement

Mollusc shells are emblematic of the morphological diversity in nature. They are important models for understanding the evolution of form; they are all variations on the same basic geometrical groundplan, their shapes can be directly related to various adaptations, and they have an exquisite fossil record. Despite these advantages, the developmental mechanisms that control shell development are unknown. We examined cell division patterns in the shell-secreting epithelium and found striking asymmetries in proliferation rate and division orientation that correlate with key aspects of shell morphogenesis in two gastropods with different shell shapes. This work provides a foundation for understanding the cellular and developmental mechanisms that generate gastropod shell form and suggest how such mechanisms might evolve to generate new morphologies.

/body

Introduction

Mollusc shells are a remarkable example of the diversity that can arise as natural selection shapes animal morphology to various ecological and functional demands. Their basic functions are structural support and protection, and shells have adapted for these roles in various ways (1–3). Soft body parts are attached to internal shell surfaces to maintain the organization of the body, and external structures can be withdrawn into shells for protection from predators or desiccation. Shell shapes often have other functions, including pelagic locomotion, burrowing, hunting, and thermal management (3–7). For these reasons, mollusc shells are important models for studying morphological evolution in extant and fossil populations (8–10).

Gastropods generally have one helically coiled shell; within that groundplan there is immense variation in shape, size, ornamentation, coiling direction, and pigmentation (Fig. 1A). Having a single shell for the lifetime of the animal often means that the same basic morphology must function over several orders of magnitude in size, from a planktonic larval stage to a large benthic animal. Gastropod shells grow by increasing their number of coils, or whorls, by exclusively growing at their aperture. A consequence of this growth pattern is that previous whorls are retained, recording the ontogenetic pattern of growth.

Despite this morphological diversity, and their utility for studies of morphological evolution, the mechanisms that underlie shell morphogenesis are not known. The differential deposition of shell material that ultimately creates shell morphology is likely driven, at least in part, by differential growth of the mantle epithelium. However, the patterns of cell division and growth of the mantle have received little attention. Some developmental regulatory genes are expressed in the mantle epithelium that generates the shell (11–16). The growth factor *dpp/BMP2-4* has been implicated in mantle proliferation (17–21). In the bivalve *Pinctada fucata*, a gradient of proliferation perpendicular to the mantle edge has been reported, with generally higher proliferation in interior parts of the mantle and lower rates in zones near the outer edges (22).

While the developmental basis of shell morphogenesis remains obscure, the process has been studied extensively using mathematical modeling. Raup (23) approximated shell shape with three different parameters: distance from axis (d), the rate of increase in each whorl's distance from the coiling axis, aperture expansion (w), the rate of aperture circumference increase, and translation (t), the rate of movement along the coiling axis (summarized in Fig. 1B). These

parameters make predictions about patterns of relative growth of the mantle that would generate different types of shells. For example, the aperture of the shell must expand to generate the basic cone shape, and in a simple Raup model of shell growth, the helical coil would be generated by greater extension at the dorsal side of the mantle aperture relative to the ventral, and greater aperture extension on the side near the apex relative to the abapical side. Such growth differences have not yet been observed at the cellular level.

Results

Organization of the larval mantle

The general anatomy of the mantle edge in adult molluscs has been described (24–26) but the larval mantle epithelium has not been examined closely. The mantle edge epithelium of the larva is organized into regular rows and regions (Fig. 2C-F). We named regions of the larval mantle based on cellular morphology, patterns of proliferation and gene expression (described below). The periostracal groove is a dominant feature of the shell margin and is clearly equivalent between larval and adult shells; this invagination secretes the chitinous, flexible periostracum, which serves as a substrate for calcium deposition and seals the biomineralizing zone off from the environment (Fig. 2). We use it as a landmark, and call the cells that form the center, lower part of the groove row 0, the anterior side row +1, and the posterior side row -1. These rows are composed of cuboidal cells with similar cell sizes in each row. Anterior to the periostracal groove rows is another row of cells, which we call the aperture growth zone (AGZ; see below). Nuclei in the AGZ are often elongated parallel to the edge of the shell. There are around 40% more cells in this row compared to the periostracal groove rows. Posterior to the periostracal groove is a region we call the mantle epithelium growth zone (MEGZ). MEGZ cells have a larger surface area than the cells of the periostracal groove and are not organized into recognizable rows. Posterior to the MEGZ is the squamous zone (SZ), where cells have a stereotypical squamous morphology. The boundary between the MEGZ and the SZ is not distinct– the cell morphologies form a continuum between these two zones.

The anterior rows of the shell margin have gene expression patterns that further support the identity of the rows as developmental and functional units (Fig. 3). We have found multiple genes that are specific to particular rows. We also observe varying periodicities in expression across the shell margin, ranging from every 1 to every 5 cells. Together, the expression patterns within and between rows likely contribute to the specific functions of particular rows.

These results show that discrete morphological zones are present in the larval mantle edge epithelium, including the periostracal groove. These correspond to regions that have been characterized in the mantle of adults (24), suggesting that the larval shell margin may be a useful model for understanding the development of the gastropod shell. Importantly, the larval shell has helicospiral growth that is geometrically similar to that of the adult (Fig. 1E).

Cell proliferation in the mantle epithelium

To investigate the differential growth of the shell margin, we labeled proliferating cells with the thymidine analog EdU, revealing high levels of division in the cells of the AGZ and MEGZ compared to other mantle epithelium regions (Fig. 4A). 20% of AGZ nuclei and 33% of MEGZ nuclei were labeled. Periostracal groove cells (rows +1, 0, and -1) showed much lower rates (2, 3, and 4%, respectively). Squamous cells were also rarely labeled (4%). This experiment

revealed high rates of division in the MEGZ and the AGZ, indicating that these regions function as growth zones in the mantle epithelium.

To follow the behavior of labeled cells we chased embryos for 4 and 8 hours after a 10-minute pulse. Labeling rates in the periostracal groove were low (3%) and did not increase during our chases. In the AGZ, the number and percentage of labeled cells increased with time (Mean values: T0: 43/215 (20%), T4: 58/255 (23%), T8: 76/190 (40%)). The same was true in the MEGZ (Mean values: T0: 92/277 (33%), T4: 160/257 (62%), T8: 188/232 (81%)) (Fig. 4B). In the squamous zone, the proportion of labeled cells increased dramatically from T0 to T4, at a much faster rate than observed in the other zones (Mean value: T0: 6/168 (4%), T4: 47/272 (17%), T8: 37/176 (21%)). We suggest that conversion of MEGZ cells to squamous cells may explain this significant labeling increase. We observed that labeled squamous cells are more often found in the anterior of the squamous region at T4 and T8, which supports this suggestion. A lower percentage of squamous cells are labeled at T8 than at T4, but not significantly so. The conversion of cuboidal cells in the MEGZ to squamous cells in the SZ could contribute to extension of the mantle epithelium, as suggested (27). In the MEGZ and AGZ the percentages of labeled cells increase with time. This indicates that the labeled cells are more likely to be dividing than their neighbors, suggesting that there are different populations of cells in each of these zones. In the MEGZ, we would expect there to be some secretory cells that are involved in biomineralization. These cells may be post-mitotic, and the proliferation we observed is from a different population of cells that drive growth of the tissue. Cather reported a non-proliferative population of cells in the *Tritia* larval mantle (28). Our data are consistent with a stem cell model, where a small number of cells divide more frequently to produce daughter cells with limited or no division, or a model where there is a population of dividing cells where both daughters of a division have similar proliferative capacities.

Orientation of cell divisions in the mantle edge

We wondered whether cell division orientation could contribute to differential growth of the mantle epithelium. To examine possible oriented cell division in *Tritia's* shell margin we analyzed fixed embryos from the above experiment (EdU pulsed for ten minutes, chased for 0, 4, and 8 hours). We identified putative sister cells and inferred their division angle relative to the anterior-posterior axis (see Methods). There are two ways in which this angle may relate to differential growth. It has been suggested that non-random polarity of cell divisions may contribute to epithelial morphogenesis (29–31). Alternatively, it has been observed that sister cells tend to align parallel to the direction of epithelial extension (32). Whether cell division angles are a cause or an effect of epithelial morphogenesis, observing a bias in the angles likely reflects the overall growth polarity of the tissue.

Different zones have different inferred cleavage orientation. In the AGZ, pairs are significantly biased to lie parallel to the shell margin (Kolmogorov-Smirnov test, $p = 0.0009$, $n = 74$ pairs; Fig. 4C). This indicates expansion of the shell margin at the aperture, one of the basic parameters of shell growth identified by modelers (*i.e.* Raup's *w*), and the first such parameter to be correlated with an aspect of cellular growth and behavior.

We next tested whether there was a left-right bias in the location of these divisions. Contrary to our prediction that most division would be on the right, we found that an excess of divisions in

the AGZ occurred on the left side of the shell margin compared to the right side (left: 35% EdU+ cells, right: 20% EdU+ cells**,** paired t-test, $p = 0.026$; Fig. 4D). This asymmetry is not predicted by basic models of shell growth but it likely underlies an underappreciated aspect of differential growth in helical gastropod shells (see Discussion).

In the MEGZ, there was a significant bias in the inferred axis of cell division, with 72% of these pairs angled to the right of the anterior-posterior axis, at an average of 27 degrees from the anterior-posterior axis (Kolmogorov-Smirnov test, $p = 0.0008$, $n = 122$ pairs; Fig. 4E). The simplest interpretation of this bias in inferred cleavage angle is the mantle on the right side more than the left. Thus, this phenomenon could explain the greater extension on the right-dorsal side of the mantle that is predicted from dextral shell morphology and incorporated in shell models. A related possibility is that there is faster secretion of periostracal membrane on the right side of the margin, which stretches the mantle in this direction, causing the observed bias in inferred cleavage orientation.

Unlike the AGZ, we found no bias in the number of divisions in the left or right MEGZ. Divisions in the SZ are, on average, right-biased 17 degrees, but not significantly so (Kolmogorov-Smirnov test, $p = 0.9412$, $n = 16$ pairs; Fig. 4G).

We wondered how division rates in the MEGZ differed along the dorsal-ventral axis of the shell margin, as differential growth between these regions may contribute to revolution around the coiling axis (similar to Raup's *d*). We examined the ventral side of the aperture and found that we could not recognize periostracal groove cells, presumably because the ventral side of the aperture is shell that was secreted in a previous whorl. Since we cannot compare ventral margin to dorsal margin, we instead compared the rates of MEGZ cell division in the dorsal, left, and right regions after an EdU pulse. As expected, labeling was highest on the dorsal mantle, but not significantly so (68% EdU+ cells in the dorsal MEGZ, 60% in the left-lateral MEGZ, and 58% in the right-lateral MEGZ: Fig. 4F). Thus, subtle differences in proliferation between the dorsal epithelium compared to the lateral regions may contribute to revolution around the coiling axis. This may be augmented by the absence of growth on the ventral part of the margin, where we were unable to see the growth zones that we recognized on the dorsal and lateral sides.

Coiling without translation in Planorbella sp.

Planispiral shells have evolved multiple times in gastropods and are also found in Nautiloids. In these shells, there is no translation of the aperture away from the apex, so that all whorls are in the same plane (Fig. 5A). We examined inferred cleavages in a planorbid to test whether the patterns we observe are associated with helical coiling. Planorbids, or ramshorn snails, are derived from snails with sinistral coiling chirality (opposite of the dextral coiling of *Tritia*), so while they are almost perfectly planispiral, they show a slight sinistral chirality. We stained and imaged planorbid pre-hatchling juveniles and observed a shell margin organization that resembled *Tritia*, allowing identification of congruent zones (Fig. 5AB). While the structures of freshwater snail shells are generally less complex than marine snails, the adult *Planorbella* shell contains three distinct crystalline layers while the *Tritia* larval shell contains one (28, 33, 34). Thus, the planorbid mantle likely has additional spatial complexity in gene expression and function that we have not yet appreciated. A pulse-fix experiment showed that most cell division was in the AGZ and the SZ (AGZ: 386/1860 (21%) MEGZ: 64/963 (7%) SZ: 55/326 (17%); Fig

5D). When comparing the number of EdU positive cells between the left and right sides of these regions, we found no bias in the MEGZ and SZ (Fig. 4E; MEGZ: left: 7% EdU+ cells, right: 6.4% EdU+ cells, paired t-test, $p = 0.635$; SZ: left: 16.7% EdU+ cells, right: 17.7% EdU+ cells, paired t-test, $p = 0.678$). In the AGZ, we found significantly higher labeling on the right-dorsal side (left: 17.6% EdU+ cells, right: 22.4% EdU+ cells, paired t-test, $p = 0.023$).

After a pulse-chase experiment (45 minute EdU pulse, zero, 4.5, and 9 hour chases) we measured the inferred division angle of sister cells. In the planorbid AGZ, MEGZ, and SZ we observed distributions of angles that are not significantly different than a null distribution. (AGZ: Kolmogorov-Smirnov test, $p = 0.3932$, $n = 162$ pairs; MEGZ: Kolmogorov-Smirnov test, $p = 0.054$, $n = 80$ pairs; SZ: Kolmogorov-Smirnov test, $p = 0.2037$, $n = 53$ pairs; Fig. 5F-H). These non-biased patterns of inferred cell division are consistent with the planispiral shell morphology found in planorbids. The overall lack of asymmetry in the MEGZ and SZ is consistent with loss of helical coiling, and the right side bias in the AGZ may reflect the vestigial sinistral morphology found in planorbids, and the asymmetry of the aperture shape (see Discussion).

Discussion

Our results show that the gastropod shell margin is complex and this organization may help to explain how the mantle contributes to shell morphology. The margin contains discrete morphological zones identifiable by cell morphology and putative function, and several of these regions display intricate spatial expression of putative regulatory factors. Two of these regions, which we call the AGZ and MEGZ, exhibit a higher level of proliferation than other shell margin zones and the division patterns within these zones may generate differential growth of the shell margin to control shell shape.

Aperture expansion

In both systems, we found significant growth in the tissue near the anterior-most edge of the margin, the AGZ. Division in this region should generally expand the circumference of the aperture (a.k.a. expansion, dilation or *w*), which generates the basic cone shape of the gastropod shell. In the *Tritia* larva, this is amplified by the biased orientation of sister cells in this zone so that they lay parallel to the margin. We did not observe this in *Planorbella* sp.; the AGZ is more structurally complex in this system, perhaps because it is an adult shell and/or because of the freshwater environment. We also note that since the shell forms a rigid circle around the margin, expansion of the margin may also contribute to aperture extension, because the enlarging shell margin no longer fits easily in the existing shell (3).

Translation, abapical expansion and the elaboration of gastropod coiling

In the simplest models of logarithmic helical shell growth, like Raup's, the aperture is circular, and does not intersect previous whorls. The translation component of coiling (movement of the aperture further from the apex), is driven by greater extension of the mantle edge on the apical side of the margin so the whole aperture grows away from the apex. In these models the dorsal edge of the mantle is at an oblique angle relative to the axis of coiling. This is observed in some shells, like those in the genera *Turritella* and *Tectarius* (see Fig. 6). The biased angle of division that we infer from sister cell positions in the MEGZ would extend the mantle edge more on the right, consistent with this type of translation.

However, in many gastropod shells, including the adult shells of whelks like *Tritia*, translation of the aperture seems to be driven by a different mode of growth. The ventral part of the aperture is formed by previous whorls and the aperture is elongated along the apical-abapical axis, with the dorsal margin more parallel to the axis of coiling compared to shells with round apertures considered above. In these shells, the component of coiling that moves the aperture away from the apex (*i.e.* translation) is driven less by greater *extension* of the mantle on the apical side, and more by differential *dilation/expansion* of the aperture on its abapical side. This has the effect of moving the abapical side of the aperture further from the apex as it coils around the main axis, generating the translation component of growth. This is reflected on shells by the difference in the apparent angle of expansion of the apical and abapical sides of the aperture, relative to the anterior edge of the shell (see Fig. 6). In principle, this pattern could be generated by even expansion across the margin, if the apical edge of the margin is more constrained from expansion, and the edge of the mantle can shift laterally so that cells underlie different longitudinal zones of the shell as they switch. This seems unlikely because there is evidence that differences between cells along the edge of the mantle generate contra-marginal features of the shell (35, 36) and these contra-marginal lines on the shell diverge more on the abapical side than on the apical side of the margin, consistent with differential expansion of the soft tissue (Fig. 6). Thus, our finding of higher aperture expansion on the left (abapical) side of the margin is consistent with this mode of helical coiling, as is the finding that there was more division on the right side than on the left in the planorbid, whose shell has a vestigial coiling direction that is sinistral, the reverse of *Tritia*. In fact, the aperture of the planorbid is asymmetrical and does appear to be expanding more on its right side, even if the overall growth of the shell stays in one plane (Fig. 5A) We note that in preliminary experiments with adult *Lymnaea stagnalis,* another gastropod whose shell is generated with this mode of translation, we found that the aperture appears to be *extending* more on the abapical side by biased cell divisions away from the apical side. It may be that different modes of asymmetric growth are used to accomplish this kind of aperture translation in different groups of snails. The larval shell of *Tritia* has an aperture that is rounder than that of the adult, and more oblique to the axis of coiling; this shell morphology may be generated by a mixture of both types of translation.

The difference between these two types of coiling has been considered before (37). Derived gastropods have elongated apertures, with the margin more parallel to the axis of coiling (lower "E-value"), and the shell being oriented more parallel to the substrate. This morphology is observed in both *Tritia* and *Lymnaea* adults (38). Vermeij (3, 37) notes that rotation in shells with higher E-values are usually generated by greater expansion of the aperture, and lower E-value shells accomplish rotation with greater extension of the margin. Our observations on aperture translation highlight a correlation of this pattern. For any point on the margin, rotational growth is orthogonal to translational growth, so in low E-value shells with elongated apertures, rotation is driven by extension and translation is driven by differential expansion, while high E-value shells would have the converse— rotation driven by expansion, and translation driven by extension.

Abapical expansion of the margin edge has been included in models of shell growth where the aperture can take on more complex shapes and sometimes grow allometrically (39–41), even if it has not been explicitly identified as an important part of the growth pattern, to our knowledge. That our results have converged with these more sophisticated shell models validates the efforts

to develop shell models that are explicitly oriented to describe growth at the mantle edge. Our finding of cellular asymmetries that could drive abapical aperture growth shows the value of integrating developmental studies with modeling to better understand the genesis of shell shapes. While various aperture growth models can generate very realistic shell morphology, there are too many degrees of freedom inherent in them to predict where in the mantle the relevant growth is occurring (38). In general, our work points to specific modes of growth that may produce the observed patterns of aperture behavior. For instance, explicitly including different rates of aperture expansion across the margin may better reflect actual growth processes (39).

Regionalized growth control in the mantle edge and the evolution of shell morphology
The mantle edge has regional specializations that control numerous aspects of shell morphology and structure. These include some fine-scale patterns that are repeated many times, like contramarginal ribs, and pigmentation patterns (35, 42). There are also larger scale regional specializations: these include the absence of periostracal groove on the ventral margin, as well as the differences in growth rates across the margin that we have discovered. Based on the available data, we propose that the mantle edge is a developmental axis, and different shell morphologies may be generated by varying the proliferation rate along this axis, changing the division angle bias, and/or tuning the relative rates of division between zones. The shells we have examined here are relatively simple; it seems likely that additional patterns of allometric growth underlie more complex shell ornamentations such as siphons and varices.

Materials and Methods:

Embryo collection, fixation, staining, and *in situ* hybridization were performed as previously described (43, 44). EdU assays were performed following manufacturer protocol, see Supporting Information for additional details (SI Appendix, Materials and Methods).

Acknowledgments

The authors thank Longjun Wu, Kim Thao Dao, and members of the Brisson lab for thoughtful discussions about this work, and Geerat Vermeij for insightful comments on this manuscript. We thank Longjun Wu for photographing the adult shells. We also thank Dan Bergstralh and Tara Finegan for statistical and figure advice. This work was supported by grants by the N.S.F. to J.D.L (IOS-1656558 and IOS-1146782).

Figure legends

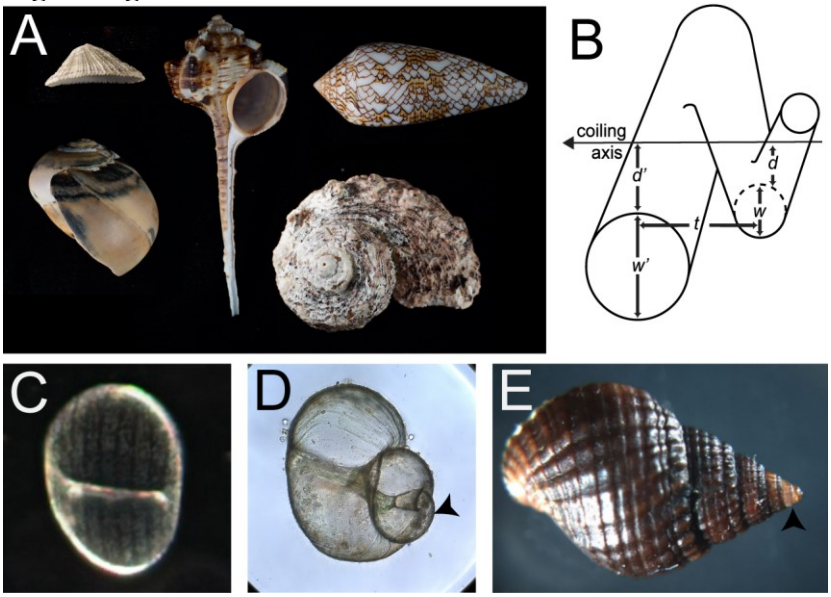

Fig. 1. Shell diversity and the whelk *Tritia obsoleta* (a.k.a. *Ilyanassa*) as a model for studies of shell development. (A) Examples of the morphological diversity of gastropod shells, listed clockwise from upper left, all measurements refer to longest photographed axis. A keyhole limpet shell (25 mm; *Diodora* sp.) viewed from the left side with the apex of the shell up and the aperture down, has no coiling and high rates of aperture expansion. A shell of *Murex* sp. (140 mm) from the aperture side, with the apex up; this shell has typical gastropod coiling, but extreme expansion of the aperture away from the apical side, producing a long siphonal process. A shell of *Conus textile* (70 mm) viewed from the side opposite the aperture, with the apex to the left. A shell of *Angaria* sp. (60 mm) viewed from the apex, with the aperture facing down. A shell of *Neverita* sp. (47 mm), with the apex up and the aperture facing to the left. (B) Simple geometrical model for shell coiling, modified from (45). The shell is modeled as a cone, growing at the open end and coiling around the main coiling axis. The rate of aperture expansion or dilation is *w;* the distance along the coiling axis traversed each rotation is *t*; the increase in distance from the coiling axis each rotation is *d.* (C) *Tritia's* right-handed larval shell at about 4.5 days old, about 125 μm wide; dorsal-posterior view, aperture is facing away from the viewer. The larval shell is made of unpigmented calcium carbonate, and lacks a prismatic nacreous layer (28). After living in the water column and developing approximately three shell whorls, the larva metamorphoses and the larval shell is retained at the juvenile shell's apex. The shell has longitudinal, contramarginal stripes, as well as periodic growth lines parallel to the aperture; these features are also present in the adult shell. (D) *Tritia* juvenile shell, shortly after metamorphosis. Shell is 350 μm wide at the aperture, first whorl at the apex is equivalent to 4.5-day-old shell (C; arrowhead). (E) *Tritia* adult shell, about 8 mm wide at the aperture's widest measurement, and 13 mm long; larval and juvenile shell are still present at the apex (black arrowhead).

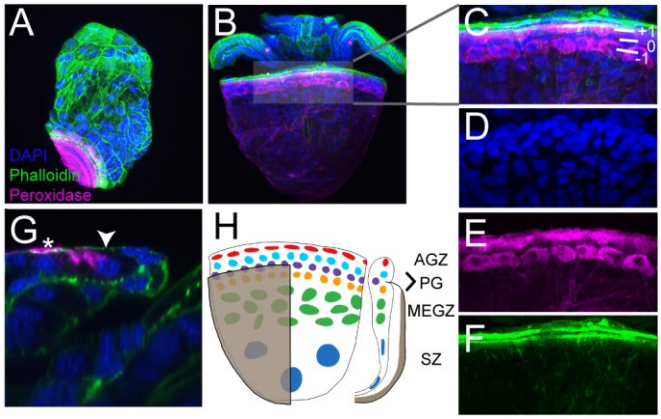

Fig. 2. Development and anatomy of the shell secreting mantle; dorsal views with anterior up unless noted; images are slab projections of confocal stacks. (A) Four-day-old embryo. The shell forms a small cup at the posterior-left side of the embryo, with its leading edge growing towards the right side. The shell's leading edge is called the aperture, where calcium is crystalized to extend the shell. Underlying the entire shell is an ectodermal tissue called the mantle epithelium. The most anterior region of the mantle epithelium is the *shell margin*, a band of cells that directly underlies the shell aperture and coordinates calcium deposition. From this stage, the shell grows more towards the anterior, so that the midline of the mantle edge comes to lie over the center of the head and the typical form of the veliger larva becomes recognizable (Fig. 2B). This reorientation is driven by the process of torsion, a morphogenetic event in gastropods that twists the posterior of the animal, including the anus, 180 degrees counterclockwise relative to the head and foot when viewed from the posterior (46, 47). Peroxidase (PO) activity is observed in the periostracal membrane that covers the shell ((48, 49), here stained with tyramide substrate in magenta). Nuclei are stained with DAPI (blue); filamentous actin is stained with phalloidin (green). (B) Seven-day-old hatchling veliger larva; velar lobes of the head are observed anterior to the shell, and eyes stain for PO (magenta). (C) is a zoom of the dorsal part of the mantle edge, as indicated, and D-F are individual channels of the merge in D. Cells of the periostracal groove are positive for PO staining (C, E). Bands of phalloidin staining are observed anterior to the groove (C, F). (G) Confocal x-z section in the sagittal plane of the mantle edge, dorsal is up, anterior is to the right. Arrowhead marks the periostracal groove, from which periostracum (asterisk) is extruded. (H) Schematic of the rows and zones of the larval mantle epithelium. Dorsal view with shell (tan) cut away on the right, and sagittal section on the right, anterior up and dorsal to the right.

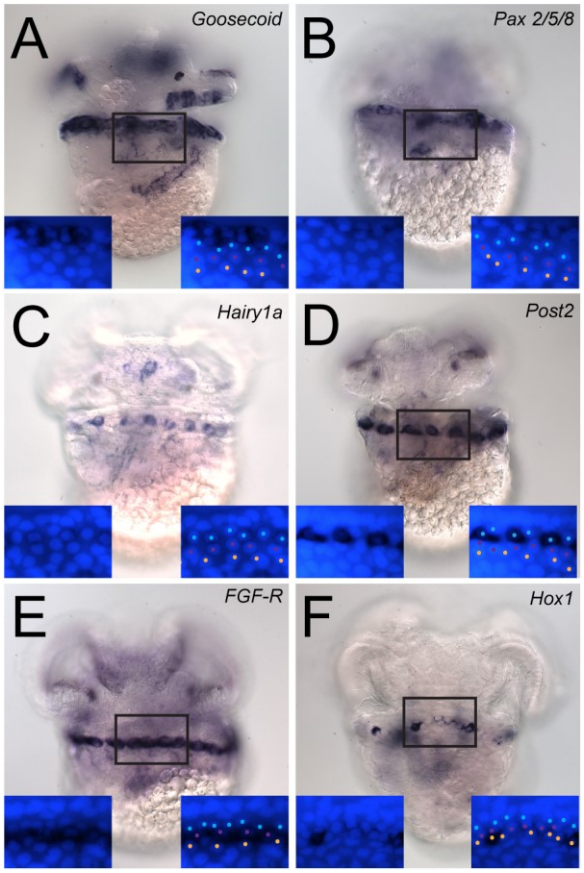

Fig. 3. Expression of putative developmental regulatory genes in the mantle epithelium. Dorsal views with anterior up, A-F are chromogenic detection of RNA *in situ* hybridization (dark blue), Insets are nuclear stainings to allow row identification (all insets are from the same embryo except C which is a different embryo from the same stage and staining experiment). The anterior (+1), middle (0) and posterior (-1) rows of the periostracal groove are marked with blue, purple and yellow dots respectively. (A) *Goosecoid* is expressed in the AGZ. (B) *Pax 2/5/8* is expressed in the AGZ. (C-D) *Hairy1a* and *Post2* are expressed in every other cell of row 0, but it is not known if they are coincident. Cell spacing in the periostracal groove is approximately the same as contramarginal stripes spacing, suggesting that stripes could be generated by cellular-scale patterning. Contramarginal stripes in the shell (See Fig. 1C) are about 2 μm wide and 17 μm apart. In fixed tissue, the underlying periostracal groove cells are separated by 12.5 μm, and cells shrink somewhat during fixation. (E) FGF-R is expressed in every cell of row 0 (F) In row -1, *Hox1* is expressed in approximately every 5 cells.

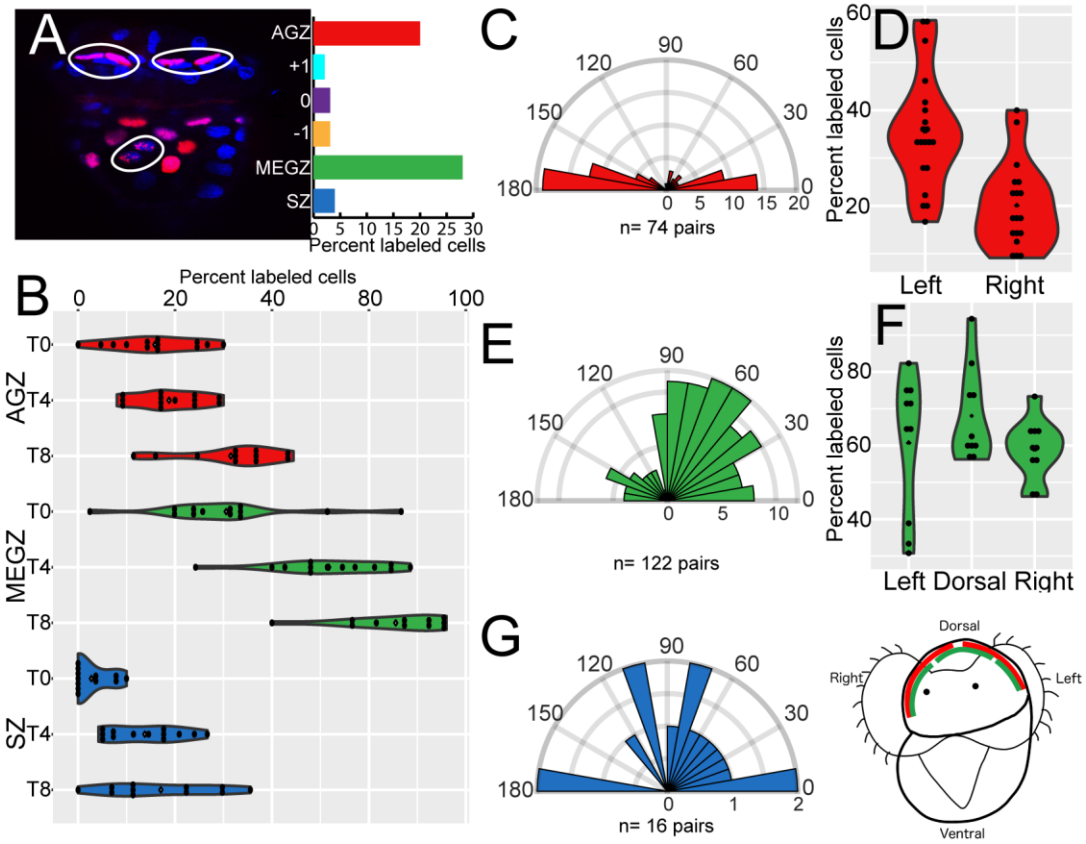

Fig. 4. Growth zones and cleavage patterns. (A) Labeling rates in mantle epithelium zones/regions. Two zones of increased proliferation are detected (AGZ and MEGZ). (B) Pulse chase EdU experiment. Moderate proliferation is detected in the AGZ over eight hours and rapid proliferation is detected in the MEGZ. (C) Division angles inferred from sister cell positions in the AGZ. Divisions are biased parallel to the shell margin. (D) Divisions are significantly more likely to occur on the left half of the AGZ. (E) Inferred division angles for MEGZ. Divisions are right biased. (F) Divisions are more frequent on dorsal MEGZ than lateral sides. (G) Inferred division angles for SZ. Divisions are not significantly biased in their direction. (H) Representative image used for inferring cleavage direction. Nuclei are stained with DAPI (blue) and EdU-positive cells contain Alexafluor 594 signal (red). Putative sister cells are circled in white.

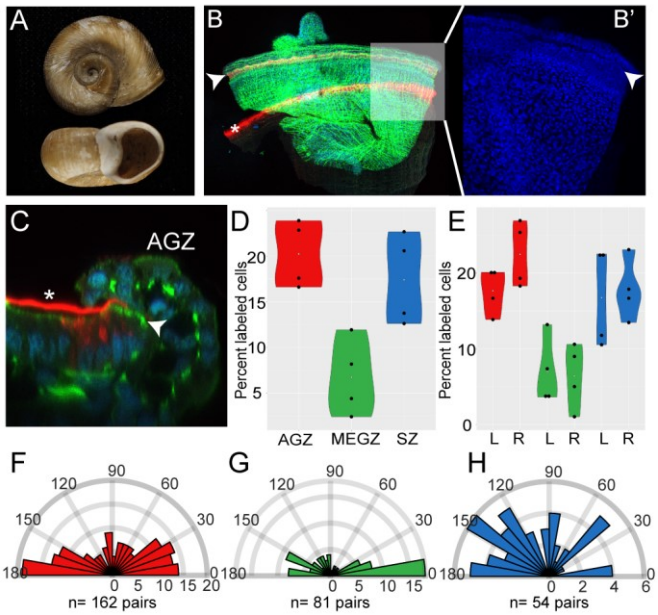

Fig. 5. Anatomy and cleavage patterns in the planorbid *Planorbella* sp. (A) *Planorbella* sp. adult shell imaged from two angles: top image shows right side, aperture is facing down, apex is in the middle of the spiral. Shell is ~10 mm in diameter. Bottom image shows view into the aperture. (B) Hatchling planorbid, nuclei are stained with DAPI (blue), actin is stained with phalloidin (green) and peroxidase is stained with tyramide substrate (red). The anterior region of peroxidase marks the periostracal groove (arrowhead) and the posterior regions marks the edge of the shell periostracum (asterisk), which has detached from the groove during processing and mounting. (B') Inset of B. The periostracal groove is indicated with arrowhead. Posterior to the groove are graded cell morphologies consistent with *Tritia's* mantle epithelium. (C) Confocal x-z section in the sagittal plane of the mantle edge, dorsal is up, anterior is to the right. PO staining is observed in the periostracal groove (arrowhead) and in the periostracal membrane (asterisk). (D) EdU pulse data. The highest rate of division is the AGZ, followed by the SZ and MEGZ. We observed no labeling in the periostracal groove. (E) AGZ labeling is significantly more frequent on the right half of the AGZ, but not in the MEGZ and SZ. (F-H) Inferred division angles for AGZ, MEGZ, and SZ. Divisions are not significantly biased in any direction.

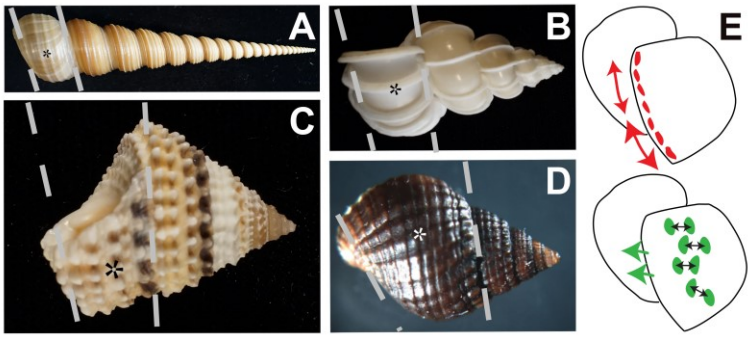

Fig. 6. Abapical growth. The apex is right for all panels. In A-D, dotted lines are shown that approximate the aperture expansion at either side of the aperture. For each, a ridge parallel to the mantle edge was selected near the front of the shell (indicated with asterisks), and the lines were placed parallel to the growth lines at the margin edges at that position. (A) A shell of *Turritella* sp., where the aperture is expanding only moderately on the abapical side. (B) A shell of *Epitonium scalare,* where the aperture is expanding similar amounts on the apical and abapical sides. (C) A shell of *Tritia obsoleta*, where the abapical side of the aperture is expanding much more than the apical side. (D) A shell of *Tectarius* sp. with a slightly greater abapical expansion. (E) Model for how the two division asymmetries found in *Tritia* could generate coiling, drawn on larval shells similar to Fig. 1D. Coiling is generated by greater aperture expansion on the abapical side (upper diagram), and greater mantle extension on the apical side (lower diagram). Higher rates of cell division on the abapical side of the AGZ, combined with a bias for these divisions to be parallel to the mantle edge, generates greater abapical expansion (red arrows). Biased cell division angles in the MEGZ are correlated with greater extension of the mantle on the apical side (green arrows).

References

1. McDougall C, Degnan BM (2018) The evolution of mollusc shells. *Wiley Interdiscip Rev Dev Biol* 7(3):e313.

2. Okabe T, Yoshimura J (2017) Optimal designs of mollusk shells from bivalves to snails. *Sci Rep* 7:42445.

3. Vermeij GJ (1993) *A Natural History of Shells* (Princeton University Press, Princeton).

4. Denny MW (2000) Limits to optimization: fluid dynamics, adhesive strength and the evolution of shape in limpet shells. *J Exp Biol* 203(Pt 17):2603–2622.

5. Denny M, Miller L (2006) Jet propulsion in the cold: mechanics of swimming in the Antarctic scallop Adamussium colbecki. *J Exp Biol* 209(22):4503–4514.

6. Levine TD, Hansen HB, Gerald GW (2014) Effects of shell shape, size, and sculpture in burrowing and anchoring abilities in the freshwater mussel Potamilus alatus (Unionidae). *Biol J Linn Soc* 111(1):136–144.

7. Palmer AR (1977) Function of Shell Sculpture in Marine Gastropods: Hydrodynamic Destabilization in Ceratostoma foliatum. *Science* 197(4310):1293–1295.

8. Gould SJ (1966) Allometry in Pleistocene Land Snails from Bermuda: The Influence of Size upon Shape. *J Paleontol* 40(5):1131–1141.

9. Lemanis R, Korn D, Zachow S, Rybacki E, Hoffmann R (2016) The Evolution and Development of Cephalopod Chambers and Their Shape. *PLOS ONE* 11(3):e0151404.

10. Ward P (1980) Comparative Shell Shape Distributions in Jurassic-Cretaceous Ammonites and Jurassic-Tertiary Nautilids. *Paleobiology* 6(1):32–43.

11. Hinman VF, O'Brien EK, Richards GS, Degnan BM (2003) Expression of anterior Hox genes during larval development of the gastropod Haliotis asinina. *Evol Dev* 5(5):508–521.

12. Jackson DJ, Degnan BM (2016) The importance of evo-devo to an integrated understanding of molluscan biomineralisation. *J Struct Biol* 196(2):67–74.

13. Lartillot N, Lespinet O, Vervoort M, Adoutte A (2002) Expression Pattern of Brachyury in the Mollusc Patella Vulgata Suggests a Conserved Role in the Establishment of the AP Axis in Bilateria. *Development* 129(6):1411–1421.

14. Lartillot N, Le Gouar M, Adoutte A (2002) Expression patterns of fork head and goosecoid homologues in the mollusc Patella vulgata supports the ancestry of the anterior mesendoderm across Bilateria. *Dev Genes Evol* 212(11):551–561.

15. Samadi L, Steiner G (2009) Involvement of Hox genes in shell morphogenesis in the encapsulated development of a top shell gastropod (Gibbula varia L.). *Dev Genes Evol* 219(9–10):523–530.

16. Wollesen T, et al. (2017) Brain regionalization genes are co-opted into shell field patterning in Mollusca. *Sci Rep* 7(1):5486.

17. Hashimoto N, Kurita Y, Wada H (2012) Developmental role of dpp in the gastropod shell plate and co-option of the dpp signaling pathway in the evolution of the operculum. *Dev Biol* 366(2):367–373.

18. Iijima M, Takeuchi T, Sarashina I, Endo K (2008) Expression patterns of engrailed and dpp in the gastropod Lymnaea stagnalis. *Dev Genes Evol* 218(5):237–251.

19. Kin K, Kakoi S, Wada H (2009) A novel role for dpp in the shaping of bivalve shells revealed in a conserved molluscan developmental program. *Dev Biol* 329(1):152–166.

20. Nederbragt AJ, van Loon AE, Dictus WJAG (2002) Expression of Patella vulgata Orthologs of engrailed and dpp-BMP2/4 in Adjacent Domains during Molluscan Shell Development Suggests a Conserved Compartment Boundary Mechanism. *Dev Biol* 246(2):341–355.

21. Shimizu K, et al. (2013) Left-right asymmetric expression of dpp in the mantle of gastropods correlates with asymmetric shell coiling. *EvoDevo* 4:15.

22. Fang Z, Feng Q, Chi Y, Xie L, Zhang R (2008) Investigation of cell proliferation and differentiation in the mantle of Pinctada fucata (Bivalve, Mollusca). *Mar Biol* 153(4):745–754.

23. Raup DM (1961) THE GEOMETRY OF COILING IN GASTROPODS. *Proc Natl Acad Sci U S A* 47(4):602–609.

24. Jackson DJ, et al. (2006) A rapidly evolving secretome builds and patterns a sea shell. *BMC Biol* 4(1):40.

25. Jolly C, et al. (2004) Zona Localization of Shell Matrix Proteins in Mantle of Haliotis tuberculata (Mollusca, Gastropoda). *Mar Biotechnol* 6(6):541–551.

26. Saleuddin ASM (1974) An electron microscopic study of the formation and structure of the periostracum in *Astarte* (Bivalvia). *Can J Zool* 52(12):1463–1471.

27. Lillie FR (1895) The embryology of the unionidae. A study in cell-lineage. *J Morphol* 10(1):1–100.

28. Cather JN (1967) Cellular interactions in the development of the shell gland of the gastropod, Ilyanassa. *J Exp Zool* 166(2):205–223.

29. Baena-López LA, Baonza A, García-Bellido A (2005) The Orientation of Cell Divisions Determines the Shape of Drosophila Organs. *Curr Biol* 15(18):1640–1644.

30. Gillies TE, Cabernard C (2011) Cell Division Orientation in Animals. *Curr Biol* 21(15):R599–R609.

31. Silva SM da, Vincent J-P (2007) Oriented cell divisions in the extending germband of Drosophila. *Development* 134(17):3049–3054.

32. Wyatt TPJ, et al. (2015) Emergence of homeostatic epithelial packing and stress dissipation through divisions oriented along the long cell axis. *Proc Natl Acad Sci* 112(18):5726–5731.

33. Marin F, Le Roy N, Marie B (2012) The formation and mineralization of mollusk shell. *Front Biosci* 4:1099–1125.

34. Wong V, Saleuddin ASM (1972) Fine structure of normal and regenerated shell of Helisoma duryi duryi. *Can J Zool* 50(12):1563–1568.

35. Boettiger A, Ermentrout B, Oster G (2009) The neural origins of shell structure and pattern in aquatic mollusks. *Proc Natl Acad Sci* 106(16):6837–6842.

36. Budd A, McDougall C, Green K, Degnan BM (2014) Control of shell pigmentation by secretory tubules in the abalone mantle. *Front Zool* 11(1):62.

37. Vermeij GJ (1971) Gastropod evolution and morphological diversity in relation to shell geometry. *J Zool* 163(1):15–23.

38. Noshita K, Shimizu K, Sasaki T (2016) Geometric analysis and estimation of the growth rate gradient on gastropod shells. *J Theor Biol* 389:11–19.

39. Checa A (1991) Sectorial expansion and shell morphogenesis in molluscs. *Lethaia* 24(1):97–114.

40. McGhee GR (1980) Shell Form in the Biconvex Articulate Brachiopoda: A Geometric Analysis. *Paleobiology* 6(1):57–76.

41. Urdy S, Goudemand N, Bucher H, Chirat R (2010) Allometries and the morphogenesis of the molluscan shell: a quantitative and theoretical model. *J Exp Zoolog B Mol Dev Evol* 314B(4):280–302.

42. Checa AG (2002) Fabricational morphology of oblique ribs in bivalves. *J Morphol* 254(2):195–209.

43. Gharbiah M, et al. (2009) The Snail Ilyanassa: A Reemerging Model for Studies in Development. *Cold Spring Harb Protoc* 2009(4):pdb.emo120.

44. Kingsley EP, Chan XY, Duan Y, Lambert JD (2007) Widespread RNA segregation in a spiralian embryo. *Evol Dev* 9(6):527–539.

45. Raup DM (1966) Geometric Analysis of Shell Coiling: General Problems. *J Paleontol* 40(5):1178–1190.

46. Garstang W (1928) The origin and evolution of larval forms. *Nature* 211:366.

47. Tomlinson SG (1987) Intermediate Stages in the Embryonic Development of the Gastropod Ilyanassa obsoleta: a Scanning Electron Microscope Study. *Int J Invertebr Reprod Dev* 12(3):253–280.

48. Hohagen J, Jackson DJ (2013) An ancient process in a modern mollusc: early development of the shell in Lymnaea stagnalis. *BMC Dev Biol* 13(1):27.

49. Timmermans LPM (1968) Studies On Shell Formation in Molluscs. *Neth J Zool* 19(4):413–523.